JLAB-THY-23-3638xxx, ADP-23-2/T1211

# Global QCD Analysis and Dark Photons

N. T. Hunt-Smith,[1] W. Melnitchouk,[1,2] N. Sato,[2] A. W. Thomas,[1] X. G. Wang,[1] and M. J. White[1]

[1] *CSSM and ARC Centre of Excellence for Dark Matter Particle Physics, Department of Physics, University of Adelaide, Adelaide 5005, Australia*
[2] *Jefferson Lab, Newport News, Virginia 23606, USA*

**Jefferson Lab Angular Momentum (JAM) Collaboration**

(Dated: January 23, 2023)

We perform a global QCD analysis of high energy scattering data within the JAM Monte Carlo framework, including a coupling to a dark photon that augments the standard model electroweak coupling via kinetic mixing with the $Z$ boson. We find a significant reduction in $\chi^2$ favoring the inclusion of a dark photon, with a statistical significance in excess of $7\sigma$, while the resulting parton distribution functions are consistent with previous global analyses within uncertainties. The modifications to the theoretical predictions are spread across a wide range of $x$ and $Q^2$, with the largest improvement corresponding to neutral current data from HERA. The best fit gives a dark photon mass in the range 3–4 GeV, and upwards of 0.1 for the mixing parameter, $\epsilon$.

*Introduction.*— Despite the enormous success of the standard model (SM) of nuclear and particle physics, it remains an incomplete theory because of its inability to explain dark matter. One relatively simple addition that could be made to at least provide a portal to the dark sector would be to introduce a new U(1) massive gauge boson [1–3], referred to as the dark photon. Here the dark photon is chosen to mix kinetically with the SM hypercharge boson, requiring an additional Lagrangian term [4],

$$\mathcal{L} \supset -\frac{1}{4}F'_{\mu\nu}F'^{\mu\nu} + \frac{m^2_{A'}}{2}A'_\mu A'^\mu + \frac{\epsilon}{2\cos\theta_W}F'_{\mu\nu}B^{\mu\nu}\,. \quad (1)$$

We use $A'$ to denote the unmixed version of the dark photon. The parameter $\epsilon$ describes the degree of mixing between the dark photon and the $B$ boson of the standard electroweak theory, $\theta_W$ is the Weinberg angle, and $F'_{\mu\nu}$ is the dark photon strength tensor. After electroweak symmetry breaking and diagonalizing the kinetic terms and gauge boson masses, three physical vectors remain which couple to the SM fermions: the massless photon $\gamma$, the massive $Z$ boson, and the physical dark photon, labelled $A_D$.

Many accelerator-based searches for $A_D$ have been undertaken [5–8], with none observing a signal to date. Large regions of parameter space with $\epsilon > 10^{-3}$ in both light and heavy mass regions have been ruled out [9], with a few gaps associated with the production of resonances, such as the $J/\psi$ and its excited states. Further competitive constraints have recently been placed on the dark photon from "decay-agnostic" (independent of decay modes or production mechanism) processes, such as the muon $g-2$ anomaly [10, 11], the electroweak precision observables (EWPO) [12, 13], $e^\pm p$ deep-inelastic scattering (DIS) [14–16], parity-violating electron scattering [17, 18], and rare kaon and $B$-meson decays [19].

The dark photon contributes to DIS processes coherently along with photon and $Z$ boson exchange, as illustrated in Fig. 1. It has also been shown to be necessary to simultaneously extract the parton distribution functions (PDFs) from the data when incorporating beyond the SM (BSM) physics into proton structure [20]. A recent exploratory study [15] included an extraction of the PDFs alongside the dark photon contribution, although that analysis limited itself to a subset of the existing HERA and BCDMS data and employed only a basic leading order (LO) parametrization of the PDFs.

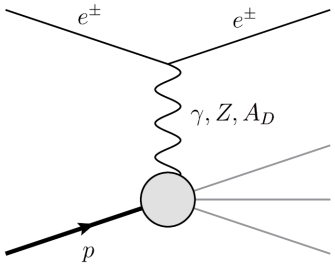


FIG. 1. Kinetic mixing of the dark photon $A_D$ with SM mediators $\gamma$ and $Z$ in $e^\pm p$ DIS [14].

In this Letter we report the first global QCD analysis including the dark photon within the JAM next-to-leading order (NLO) analysis framework. This approach employs modern Monte Carlo techniques and state-of-the-art uncertainty quantification, taking into account power corrections and nuclear effects with nucleon off-shell corrections [21]. We simultaneously determine the optimum set of PDFs, as well as the preferred dark photon parameters, and also perform a hypothesis test against the SM. The result of this analysis is an improvement of more than $7\sigma$ in the global fit when a dark photon is included.

*Dark photon background.*— The $F_2$ proton structure function, including the dark photon, is given by [14]

$$\widetilde{F}_2 = \sum_{i,j=\gamma,Z,A_D} \kappa_i \kappa_j F_2^{ij}, \quad (2)$$

where $\kappa_i = Q^2/(Q^2+m_i^2)$. At LO in $\alpha_s$, one has

$$F_2^{ij} = \sum_q (C_{i,e}^v C_{j,e}^v + C_{i,e}^a C_{j,e}^a)(C_{i,q}^v C_{j,q}^v + C_{i,q}^a C_{j,q}^a)\, x f_q, \tag{3}$$

where $x$ is the parton momentum fraction, and $f_q$ is the PDF for quark flavor $q$ in the proton. The vector and axial vector couplings to the electron and quarks for the photon are

$$\{C_{\gamma,e}^v, C_{\gamma,u}^v, C_{\gamma,d}^v\} = \left\{-1, \frac{2}{3}, -\frac{1}{3}\right\}, \qquad C_\gamma^a = 0, \tag{4}$$

while for the unmixed $Z$ boson the couplings are

$$\overline{C}_Z^v \sin 2\theta_W = T_3^f - 2q_f \sin^2\theta_W, \quad \overline{C}_Z^a \sin 2\theta_W = T_3^f, \tag{5}$$

where $T_3^f$ is the third component of the weak isospin, and $q_f$ the electric charge. After diagonalizing the mixing term through field redefinitions, the couplings of the physical $Z$ and $A_D$ to SM particles are given by [14]

$$\begin{aligned} C_Z^v &= (\cos\alpha - \epsilon_W \sin\alpha)\, \overline{C}_Z^v + \epsilon_W \sin\alpha \cot\theta_W\, C_\gamma^v, \\ C_Z^a &= (\cos\alpha - \epsilon_W \sin\alpha)\, \overline{C}_Z^a, \end{aligned} \tag{6}$$

and

$$\begin{aligned} C_{A_D}^v &= -(\sin\alpha + \epsilon_W \cos\alpha)\, \overline{C}_Z^v + \epsilon_W \cos\alpha \cot\theta_W C_\gamma^v, \\ C_{A_D}^a &= -(\sin\alpha + \epsilon_W \cos\alpha)\, \overline{C}_Z^a, \end{aligned} \tag{7}$$

Here $\alpha$ is the $\bar{Z}$–$A'$ mixing angle,

$$\begin{aligned} \tan\alpha = \frac{1}{2\epsilon_W}\Big[1 - \epsilon_W^2 - \rho^2 \\ - \text{ sign}\,(1-\rho^2)\sqrt{4\epsilon_W^2 + (1-\epsilon_W^2-\rho^2)^2}\Big], \end{aligned} \tag{8}$$

with $\epsilon_W$ given in terms of the free mixing parameter $\epsilon$,

$$\epsilon_W = \frac{\epsilon \tan\theta_W}{\sqrt{1 - \epsilon^2/\cos^2\theta_W}}, \tag{9}$$

and $\rho$ is defined by

$$\rho = \frac{m_{A'}/m_{\bar{Z}}}{\sqrt{1-\epsilon^2/\cos^2\theta_W}}. \tag{10}$$

The physical masses of the $Z$ boson and dark photon then become

$$\begin{aligned} m_{Z,A_D}^2 = \frac{m_{\bar{Z}}^2}{2}\Big[1 + \epsilon_W^2 + \rho^2 \\ \pm \text{ sign}\,(1-\rho^2)\sqrt{(1+\epsilon_W^2+\rho^2)^2 - 4\rho^2}\Big], \end{aligned} \tag{11}$$

with $\bar{Z}$ the unmixed version of the SM neutral weak boson. In our analysis we include the two dark parameters $\epsilon$ and the mass $m_{A_D}$ in the fitting parameters.

*Methodology.*— Our baseline study uses the JAM QCD analysis framework, employing Monte Carlo sampling and NLO perturbative QCD corrections (see Ref. [21] for details). To accurately characterize the PDFs and their uncertainties, the global analysis was performed 200 times using data resampling, repeatedly fitting to data that were distorted by Gaussian shifts within their quoted uncertainties. The resulting replica sets approximate Bayesian samples of the posterior, from which one constructs uncertainty bands [22]. Each individual fit determines 30 free proton PDF parameters, along with 6 parameters for higher twists and 6 for nucleon off-shell corrections. Starting from the best fit replicas of the previous JAM analysis [21], our global analysis incorporates the JAM multi-step strategy, whereby data are gradually added one step at a time, as an efficient way of honing in on the global minimum.

The minimization of the $\chi^2$ begins with fixed target DIS data from SLAC [23], BCDMS [24], and NMC [25, 26], and DIS data from the HERA collider [27]. Drell-Yan data from the Fermilab NuSea [28] and SeaQuest [29] experiments are then added and the $\chi^2$ minimization procedure repeated using the previous best fit parameters as a starting point. Subsequent steps include the addition of $Z$-boson rapidity data [30, 31], followed by $W$-asymmetry data [32, 33], and finally jet production data from $p\bar{p}$ collisions [34, 35]. For all datasets, a $Q^2$ cut of 1.69 GeV$^2$ and a $W^2$ cut of 10 GeV$^2$ were employed, as in Ref. [21]. The fit that minimized the total $\chi^2$ was identified as the default or baseline fit.

The modifications required to include the effects of the dark photon were then added to the underlying JAM theory, allowing the two additional dark parameters $m_{A_D}$ and $\epsilon$ to be fitted alongside the PDF parameters. After repeating the 200 global fits from the same starting points, the best fit was identified for the dark photon.

*Global fit results.*— A comparison of the $\chi^2$ per datum between the baseline best fit and the dark photon best fit for the different datasets included is given in Table I. There is a clear improvement in the $\chi^2$ for the fixed target DIS and HERA neutral current (NC) datasets with the inclusion of the dark photon. Although all the other datasets have a higher $\chi^2$ with the dark photon, no mod-

TABLE I. Comparison of the minimum $\chi^2$ values per datum, $\chi^2_{\rm min}$, with ("dark") and without ("base") dark photon modifications for various datasets.

| reaction | $\chi^2_{\rm min}$(dark) | $\chi^2_{\rm min}$(base) | $N_{\rm dat}$ |
|---|---|---|---|
| fixed target DIS | 1.026 | 1.046 | 1495 |
| HERA NC | 1.215 | 1.262 | 1104 |
| HERA CC | 1.173 | 1.143 | 81 |
| Drell-Yan | 1.206 | 1.143 | 205 |
| $Z$ rapidity | 1.068 | 1.059 | 56 |
| $W$ asymmetry | 0.850 | 0.810 | 97 |
| jets | 1.229 | 1.205 | 200 |
| **total** | 1.098 | 1.117 | 3283 |

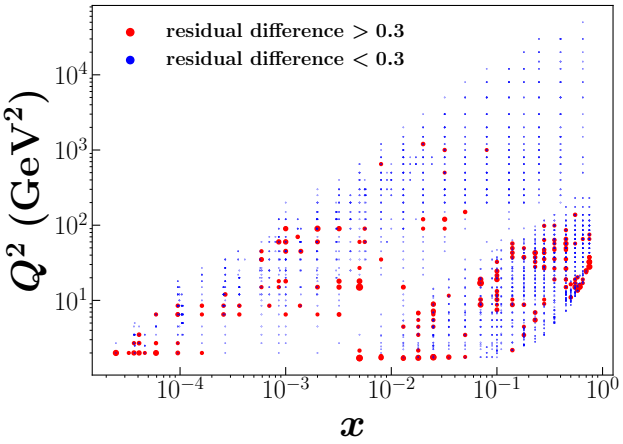


FIG. 2. Points in DIS kinematics $(Q^2, x)$ exhibiting the greatest difference in residuals ($> 0.3$ in red, $< 0.3$ in blue) between dark and baseline best fits.

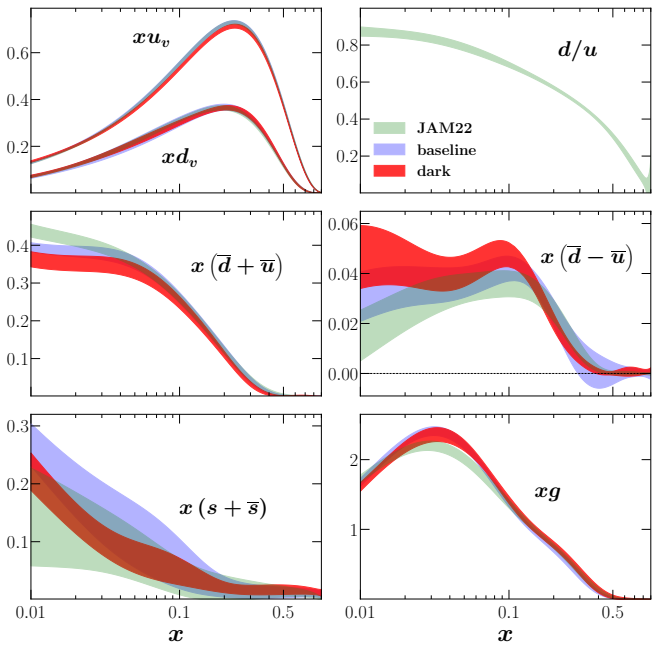


FIG. 3. PDFs comparing best fit with ("dark", red bands) and without ("baseline", blue bands) the dark photon modifications to the JAM22 global analysis (green bands) at the input scale, $Q^2 = 1.69$ GeV$^2$.

ifications have been made to the underlying theory for these reactions, so we do not expect any improvement. The sheer number of NC DIS data points means that the total $\chi^2$ still shows a substantial improvement; applying Wilks' theorem, the difference in total $\chi^2$ corresponds to a $p$-value of $\sim 3.8 \times 10^{-14}$ or $\sim 7.5\sigma$.

There is no localized region of kinematics which contains the greatest difference in residuals, as can be seen in Fig. 2. The marker size of the data points corresponds to the absolute value of the difference in residuals, with values less than 0.3 set to a very small size and shown in blue. The theory predictions with the greatest modifications tend to be located at low to intermediate values of $Q^2$, however, there is no clear $x$ dependence.

In Fig. 3 we compare the PDFs from the dark best fit and the most recent JAM22 unpolarized PDF results [21]. The dark PDFs overlap with the JAM22 PDF uncertainty bands most of the time, particularly for the valence quark distributions that are the most well-constrained by existing data. This suggests that the dark photon results are indeed consistent with existing PDF analyses. The baseline fit is similarly close to the previous JAM analysis, which provides a further consistency check.

Of course, it is possible that the additional degrees of freedom that have been added into the underlying theory may be compensating for some aspect of the QCD theory currently missing in the global analysis, such as higher order QCD corrections. The inclusion of next-to-next-to-leading order (NNLO) effects, for instance, has been shown to improve the fit for HERA datasets to a similar extent as observed by adding the dark photon modifications [36]. On the other hand, there are significant differences between the reduction in $\chi^2$ reported here and that arising from NNLO corrections, with the data points showing the greatest reduction in residuals for the dark photon spread across $x$ and $Q^2$, as opposed to NNLO, where the improvements are expected to be isolated to particular kinematic regions. We also see no improvement in $\chi^2$ for charged current DIS with the dark photon, whereas the NNLO fit improves significantly for those datasets. Furthermore, within the HERA NC datasets there are significant improvements for the dark photon that are not present in NNLO, and vice versa. Finally, the fixed target DIS also shows a large improvement in $\chi^2$ for the dark photon.

We also checked the validity of applying Wilks' theorem to our results, using the data resampling method. This confirmed that we do indeed have a $\chi^2$-distributed log-likelihood ratio, implying that the $p$-value quoted above should be a good approximation.

In the same way as the replica samples allow uncertainties on the PDF parameters to be computed, variation in the optimized dark photon parameters associated with the shuffling of the data can provide uncertainties on these too. Figure 4 illustrates the replica samples, with contours indicating 1, 1.5 and $2\sigma$ levels. The ranges of the dark parameters favored by the data give for a dark photon mass $m_{A_D} = 3.47 \pm 0.49$ GeV and mixing parameter $\epsilon = 0.144 \pm 0.016$, at 68% confidence level. This value of the mixing parameter appears rather high, as $\epsilon > 10^{-3}$ has been largely excluded for a wide range of mass values [9]. On the other hand, there do exist regions of parameter space within this mass range which cannot be excluded because of the presence of other particles, notably the $J/\psi$ and its excited states. The preferred

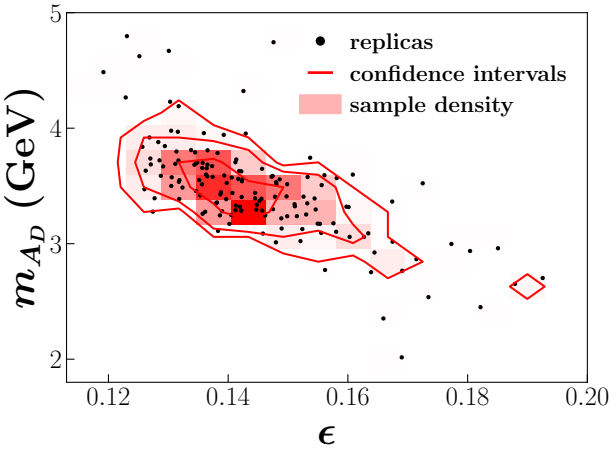


FIG. 4. Replica samples of dark parameters for the dark photon mass $m_{A_D}$ versus the mixing parameter $\epsilon$. The red contours denote 1, 1.5 and 2 $\sigma$ confidence levels and the red shaded regions show the sample density.

value for the dark photon mass has an uncertainty range wide enough to encompass these unconstrained regions, meaning that our fitted values for the dark parameters are not inconsistent with existing experiments.

*Outlook.*— In summary, our analysis has revealed a strong indication of the existence of a new BSM particle, the dark photon. The statistical significance of this result suggests an urgent need for further tests to confirm this finding. In the future, since nucleon PDFs are the input in determinations of many physical quantities, such as the $W$-boson mass [37] or the weak couplings [38], it will be important to apply the PDFs from the dark best fit to re-extract these quantities.

This work was supported by the DOE contract No. DE-AC05-06OR23177, under which Jefferson Science Associates, LLC operates Jefferson Lab; and by the University of Adelaide and the Australian Research Council through the ARC Centre of Excellence for Dark Matter Particle Physics (CE200100008) and Discovery Project DP180102209 (MJW).

[1] P. Fayet, Phys. Lett. B **95**, 285 (1980).
[2] P. Fayet, Nucl. Phys. B **187**, 184 (1981).
[3] B. Holdom, Phys. Lett. B **166**, 196 (1986).
[4] L. B. Okun, Sov. Phys. JETP **56**, 502 (1982).
[5] J. P. Lees *et al.*, Phys. Rev. Lett. **119**, 131804 (2017), arXiv:1702.03327 [hep-ex].
[6] D. Banerjee *et al.*, Phys. Rev. Lett. **123**, 121801 (2019), arXiv:1906.00176 [hep-ex].
[7] R. Aaij *et al.*, Phys. Rev. Lett. **124**, 041801 (2020), arXiv:1910.06926 [hep-ex].
[8] A. M. Sirunyan *et al.*, Phys. Rev. Lett. **124**, 131802 (2020), arXiv:1912.04776 [hep-ex].
[9] M. Graham, C. Hearty, and M. Williams, Ann. Rev. Nucl. Part. Sci. **71**, 37 (2021), arXiv:2104.10280 [hep-ph].
[10] M. Pospelov, Phys. Rev. D **80**, 095002 (2009), arXiv:0811.1030 [hep-ph].
[11] H. Davoudiasl, H.-S. Lee, and W. J. Marciano, Phys. Rev. Lett. **109**, 031802 (2012), arXiv:1205.2709 [hep-ph].
[12] A. Hook, E. Izaguirre, and J. G. Wacker, Adv. High Energy Phys. **2011**, 859762 (2011), arXiv:1006.0973 [hep-ph].
[13] D. Curtin, R. Essig, S. Gori, and J. Shelton, JHEP **02**, 157 (2015), arXiv:1412.0018 [hep-ph].
[14] G. D. Kribs, D. McKeen, and N. Raj, Phys. Rev. Lett. **126**, 011801 (2021), arXiv:2007.15655 [hep-ph].
[15] A. W. Thomas, X. G. Wang, and A. G. Williams, Phys. Rev. D **105**, L031901 (2022), arXiv:2111.05664 [hep-ph].
[16] B. Yan, Phys. Lett. B **833**, 137384 (2022), arXiv:2203.01510 [hep-ph].
[17] A. W. Thomas, X. G. Wang, and A. G. Williams, Phys. Rev. Lett. **129**, 011807 (2022), arXiv:2201.06760 [hep-ph].
[18] A. W. Thomas and X. G. Wang, Phys. Rev. D **106**, 056017 (2022), arXiv:2205.01911 [hep-ph].
[19] H. Davoudiasl, H.-S. Lee, and W. J. Marciano, Phys. Rev. D **85**, 115019 (2012), arXiv:1203.2947 [hep-ph].
[20] S. Carrazza, C. Degrande, S. Iranipour, J. Rojo, and M. Ubiali, Phys. Rev. Lett. **123**, 132001 (2019), arXiv:1905.05215 [hep-ph].
[21] C. Cocuzza, W. Melnitchouk, A. Metz, and N. Sato, Phys. Rev. D **104**, 074031 (2021), arXiv:2109.00677 [hep-ph].
[22] N. T. Hunt-Smith, A. Accardi, W. Melnitchouk, N. Sato, A. W. Thomas, and M. J. White, Phys. Rev. D **106**, 036003 (2022), arXiv:2206.10782 [hep-ph].
[23] L. W. Whitlow, E. M. Riordan, S. Dasu, S. Rock, and A. Bodek, Phys. Lett. B **282**, 475 (1992).
[24] A. C. Benvenuti *et al.*, Phys. Lett. B **223**, 485 (1989).
[25] M. Arneodo *et al.*, Nucl. Phys. **B483**, 3 (1997), arXiv:hep-ph/9610231.
[26] M. Arneodo *et al.*, Nucl. Phys. **B487**, 3 (1997), arXiv:hep-ex/9611022.
[27] H. Abramowicz *et al.*, Eur. Phys. J. C **75**, 580 (2015), arXiv:1506.06042 [hep-ex].
[28] R. S. Towell *et al.*, Phys. Rev. D **64**, 052002 (2001), arXiv:hep-ex/0103030.
[29] J. Dove *et al.*, Nature **590**, 561 (2021), [Erratum: Nature **604**, E26 (2022)], arXiv:2103.04024 [hep-ph].
[30] T. A. Aaltonen *et al.*, Phys. Lett. B **692**, 232 (2010), arXiv:0908.3914 [hep-ex].
[31] V. M. Abazov *et al.*, Phys. Rev. D **76**, 012003 (2007), arXiv:hep-ex/0702025.
[32] T. Aaltonen *et al.*, Phys. Rev. Lett. **102**, 181801 (2009), arXiv:0901.2169 [hep-ex].
[33] V. M. Abazov *et al.*, Phys. Rev. Lett. **112**, 151803 (2014), [Erratum: Phys. Rev. Lett. **114**, 049901 (2015)], arXiv:1312.2895 [hep-ex].
[34] A. Abulencia *et al.*, Phys. Rev. D **75**, 092006 (2007), [Erratum: Phys. Rev. D **75**, 119901 (2007)], arXiv:hep-ex/0701051.
[35] V. M. Abazov *et al.*, Phys. Rev. D **85**, 052006 (2012), arXiv:1110.3771 [hep-ex].
[36] L. A. Harland-Lang, A. D. Martin, P. Motylinski, and R. S. Thorne, Eur. Phys. J. C **76**, 186 (2016), arXiv:1601.03413 [hep-ph].
[37] J. Gao, D. Liu, and K. Xie, Chin. Phys. C **46**, 123110 (2022), arXiv:2205.03942 [hep-ph].
[38] D. Wang *et al.*, Nature **506**, 67 (2014).